Transactions of the 17th International Conference on
Structural Mechanics in Reactor Technology (**SMiRT 17**)
Prague, Czech Republic, August 17 –22, 2003

Paper # K08-2

Experimental Studies of Free-Standing Spent Fuel Storage Cask subjected to Strong Earthquakes

Koji SHIRAI[1)], Kazuta HIRATA[1)], Toshiari SAEGUSA[1)]

[1)] Central Research Institute of Electric Power Industry (CRIEPI), Chiba, Japan

ABSTRACT

Concrete cask spent fuel storage system is considered to essentially have an economical advantage and becoming widely used. For vertically free-standing concrete cask on the floor pad in the cask storage facility, its tipping-over and sliding behavior during earthquake is one of the technical key issues to guarantee its safe performance. In this paper, the experimental studies are reported by performing the excitation test with a scale model concrete cask using two-dimensional shaking table and the applicability of the energy spectrum approach is discussed.

KEY WORDS: spent fuel, dry storage, storage facility, economical advantage, concrete cask, free-standing, earthquake, excitation test, shaking table, tipping-over, sliding, energy spectrum

INTRODUCTION

In Japan, there are sixteen sites of nuclear power stations (Light Water Reactors). At present, the rate of spent fuel arising is 900tU/a and the rate for the years 2010 will be some 1,400tU/a. At many sites, the amount of stored spent fuel is reaching the controlled-capacity. In 2011, 3,900tU of spent fuel will have to be stored away from reactor site (AFR storage), and 7,700tU will have to be stored in 2021. Therefore, it is very important issue to introduce such interim spent fuel storage facilities by around 2010.

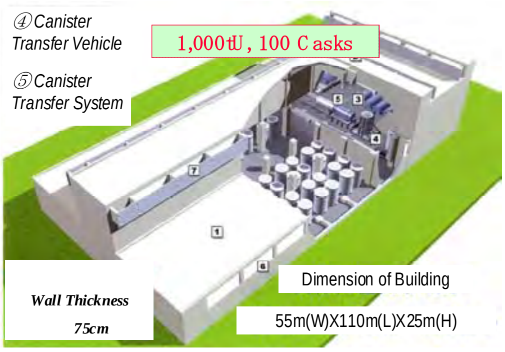

For the spent fuel storage, the dry storage with metal cask or the wet storage have been used world-widely. Recently, due to the economical reason, the concrete modular storage technology, such as concrete cask, concrete silo, is also becoming widely used. Fig.1 shows the schematic view of storage house with the concrete cask. In 2000, CRIEPI had started a program of demonstrations for determining concrete cask performance (see Fig.2) with the aim of developing “safety standards for concrete modular structures, systems and components”.

As the concrete cask will be preferable to be oriented vertically in the freestanding condition, it is very important to evaluate the tipping-over phenomena under strong earthquake motion [1]. In this study, the experimental studies are reported by performing the excitation test with a scale model concrete cask using two-dimensional shaking table test, and the applicability of the energy spectrum approach is also discussed.

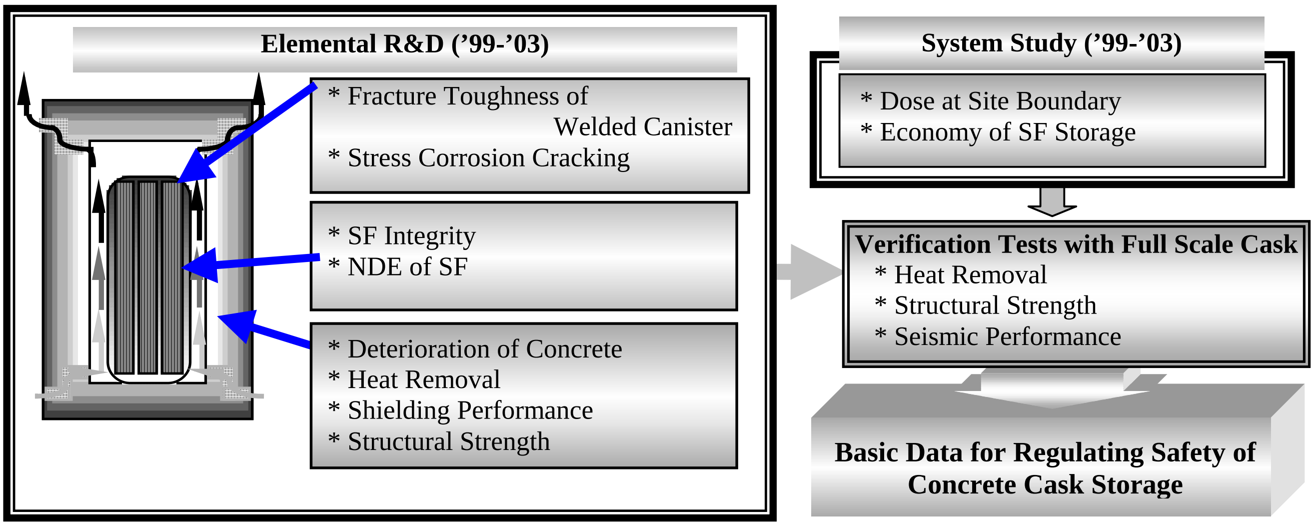

Fig. 2 Schematic showing performance of concrete cask components in dry storage
(This program is executed under contract from the Ministry of Economy, Trade and Industry).

SHAKING TABLE TEST

Prototype Cask

Japanese prototype of concrete cask assumed to be for indoor use as shown in Fig.2 is basically designed, especially considering long-term integrity of concrete materials, the restraint of cracking due to thermal stress and the improvement shielding ability. This cask consists of the storage container and the canister. The storage container is made from reinforced concrete, which becomes a structure strength part to the assumed load. The canister, which can store 21 PWR spent fuels, is a structure in which the basket is fixed by inserting a corner pipe known as a guide tube in the spacer plates, and is made from stainless steel and combines with the storage container. The canister body uses corrosion-resistant material for greater durability [2].

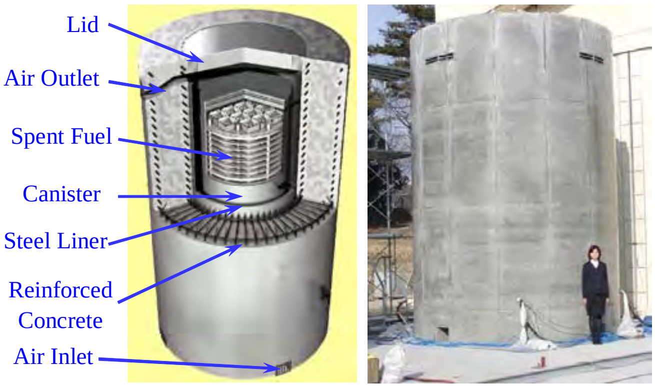

Fig.2. Japanese type of reinforced concrete cask

Scale Model Cask

The scale model cask and model floor were set on a two-dimensional (horizontal and vertical) shaking table as shown in Fig.3. A similarity law was considered in this model to simulate the effect of the gravitational acceleration on the tipping-over condition of the cask. The similarity law governing the model was summarized as shown in Table 1. The scaling ratios for acceleration, geometry and bottom stress were set to 1, 1/3, 0.95, respectively.

A 30cm thick reinforced concrete slab was used as the floor model. A scale model cask, which consists of the cask body part (including bottom part) and the canister model, was fabricated based on the similarity law referring the configuration of the prototype cask.

Table 2 shows the comparison of specifications between the prototype cask and the scale model cask. Fig.4 and Fig.5 shows the outline of the scale canister model and the scale model cask during excitation test.

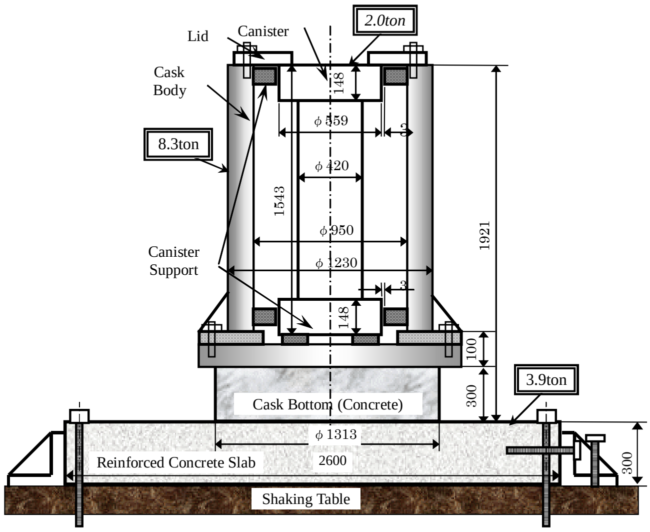

Fig.3 Scale Model Cask

Table 1. Similarity Law

Parameter	Notation	Dimension	Similarity Ratio	
			General Form*	for N=3
Length	L	L	$L_m/L_p = 1/N$	1/3
Time	T	T	$T_m/T_p = 1/N^{1/2}$	1/1.73
Acceleration	a	LT^{-2}	$a_m/a_p = 1$	1
Velocity	V	LT^{-1}	$V_m/V_p = 1/N^{1/2}$	1/1.73
Angle	θ	---	$\Theta_m/\theta_p = 1$	1
Mass	M	M	$M_m/M_p = \alpha/N^3$	0.0556
Moment of Inertia	I	ML^2	$I_m/I_p = M_mL_m^2/M_pL_p^2 = \alpha/N^5$	0.00617
Longitudinal Stiffness	K	MT^{-2}	$K_m/K_p = \beta/N$	1.02
Equivalent Cross Section	A	L^2	$A_m/A_p = \gamma/N^2$	0.144
Bottom Stress	σ	$ML^{-1}T^{-2}$	$\sigma_m/\sigma_p = (F_m/A_m)/(F_p/A_p)$	0.951
Longitudinal Force	F	MLT^{-2}	$F_m/F_p = (\alpha\beta)^{1/2} \cdot N^{-5/2}$	0.137
Friction Coefficient	u	---	$u_m/u_p = 1$	1

Note
* Suffix p denotes the prototype, and suffix m denotes the scale model
** Correction factor : for mass α = 1.50, for longitudinal stiffness β = 3.06, for mass γ = 1.30

Table 2. Comparison of specification between prototype RC cask and scale model cask

Part		Prototype cask	Scale model cask
Cask Body (including bottom part)	Outer Diameter	3.940 mm	1.230 mm
	Inner Diameter	1.850 mm	952 mm
	Height	5.787 mm	1.901 mm
	Mass	147 ton	8.17 ton
Canister	Diameter	1.676 mm	559 mm
	Height	4.630 mm	1.543 mm
	Mass	35 ton (with spent fuel)	1.95 ton

Fig.4 Canister Model

Fig.5 Scale Model Cask during the excitation test

Measuring Items

Fig.6 shows the measuring positions during the seismic excitation test. The angular velocity ω(x), ω(y), acceleration A(x), A(z) and displacement D(x), D(z) of the cask body and the canister were measured. The rotational angle was obtained by integrating the angular velocity mathematically.

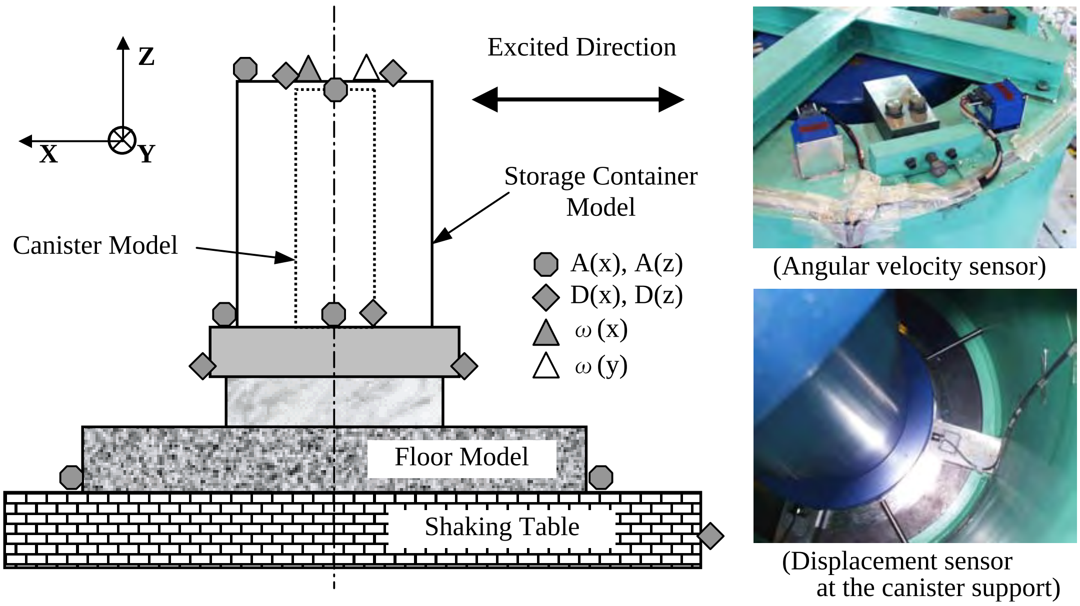

Fig.6 Measuring positions during the seismic excitation test

Test Conditions

For input of the seismic excitation test, two recorded waves during typical natural earthquake waves (El Centro, JMA Kobe) and two artificial seismic waves (Type1, Type2) were employed. Fig.7 and Fig.8 shows the time histories and acceleration response spectrum (dumping factor 5%) of the recorded waves and artificial waves, respectively.

In the excitation test, time duration of the input wave was scaled according to a similarity law shown in Table 1 and the acceleration levels were varied according to the test conditions. Test condition includes the cases considering horizontal and vertical motions simultaneously. Moreover, the effect of the gap distance between the canister model and the cask body on the overall response of the scale model cask was also investigated.

Table 3. Input waves for the seismic excitation test

Input Wave		Remarks	Max. Acc. Value
Natural Earthquake Waves	El Centro	Imperial Valley Earthquake, 1940	NS 342 gal, UD 206 gal
	JMA Kobe	Hyogo-ken Nanbu Earthquake, 1995	NS 821 gal, UD 333 gal
Artificial Seismic Waves	Type 1	Magnitude 6.5, Epicenter distance 7.2 km	H 259 gal, UD 168 gal
	Type 2	Magnitude 8.5, Epicenter distance 68 km	H 204 gal, UD 124 gal

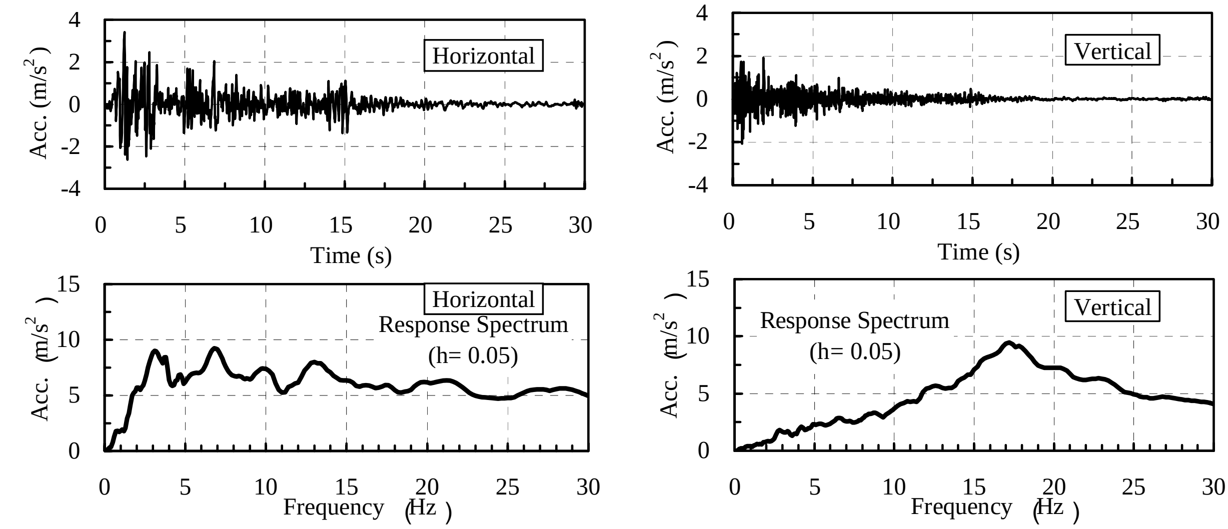

(El Centro)

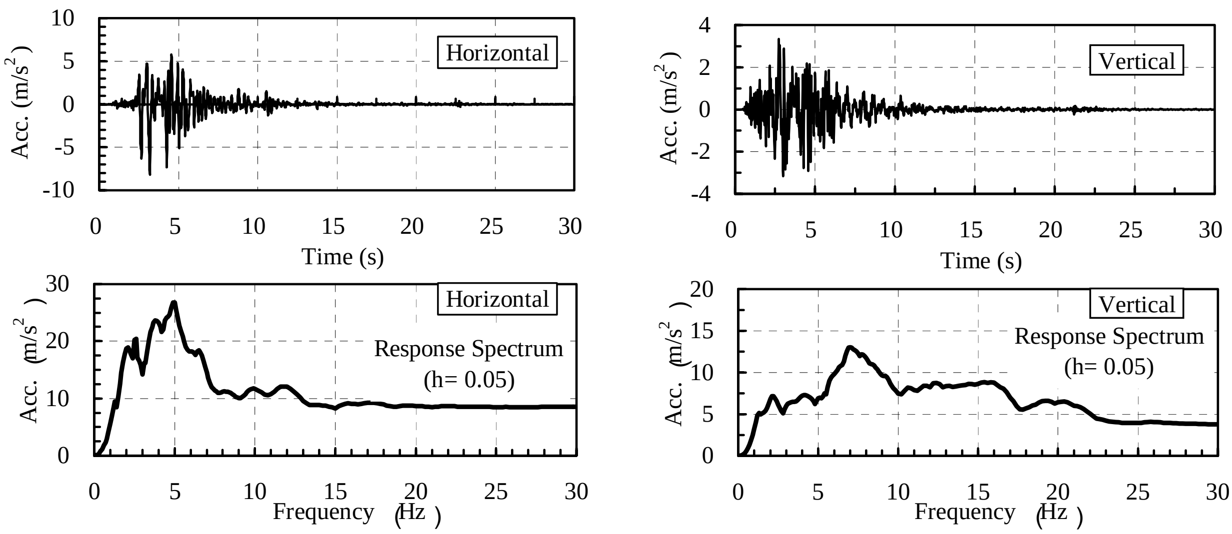

(JMA Kobe)

Fig.7 Time histories and acceleration response spectrum of the recorded waves

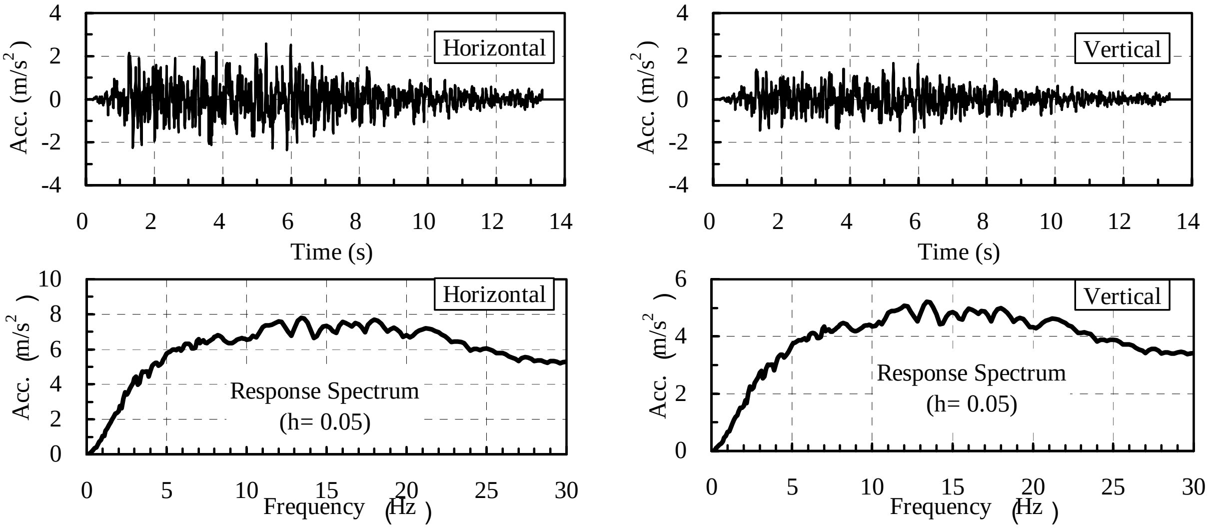

(Type 1)

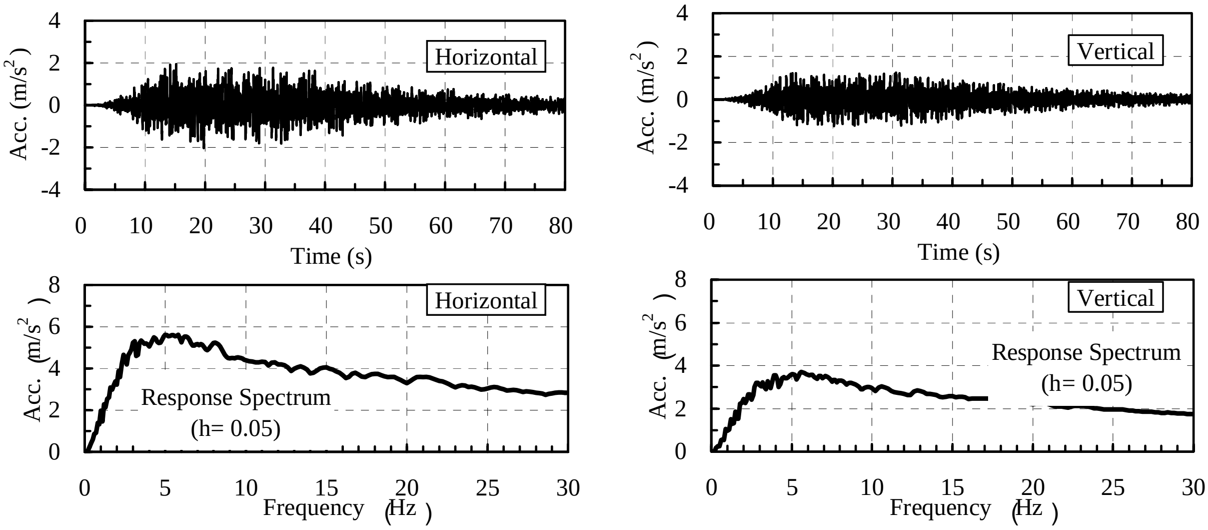

(Type 2)

Fig.8 Time histories and response spectrum of the artificial waves

TEST RESULTS

Rocking Restitution Coefficient and Kinetic Coefficient Friction

Before the shaking table test, the rocking restitution coefficient and kinetic coefficient friction between the scale model cask and the model floor were measured. In this test, there was no gap between the canister model and the cask body.

The rocking restitution coefficient δ was assumed to be the damping ratio of the maximum angular velocity obtained from a free rocking vibration test. This value is defined by equation (1) [3].

$$\dot{\theta} \rightarrow \delta \times \dot{\theta} \quad at\ t = 0 \quad (0 \le \delta \le 1)$$
$$h = \sqrt{(\ln \delta)^2 / \pi^2 + (\ln \delta)^2} \qquad (1)$$

Fig.9 shows the example of the measured time history of the angular velocity during the free rocking vibration test when the uplifting displacement at the end-point of the bottom part of the model cask was set to 40mm. The mean measured δ value was about 0.81, so the damping ratio h for the rocking vibration was calculated to be 0.066 by equation (1).

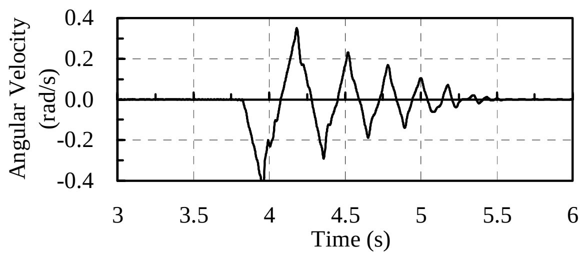

Fig.9 Example of the free rocking vibration test results

To obtain the kinetic coefficient friction between the surface of the bottom part and the concrete surface of the model floor, the sinusoidal wave excitation test using the bottom part (concrete circular plate attached to the cask body) was performed as shown in Fig.10. The kinetic coefficient friction value is defined by the ratio of the maximum acceleration measured on the bottom plate to the maximum acceleration value of the input wave.

Fig.11 shows the example of the measured time history of the coefficient friction value during the sinusoidal wave excitation test in case of frequency 5Hz. As there was no significant difference between the static coefficient and the kinetic one, the friction coefficient can be assumed to be constant and set to about 0.7.

Fig.10 Sinusoidal wave excitation test with the bottom part (f=5Hz)

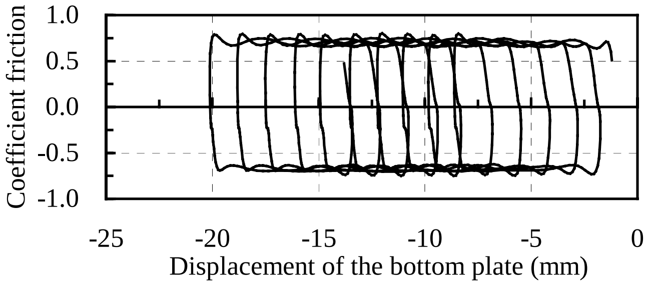

Fig.11 Sinusoidal wave excitation test results

Rocking Response

Fig.12 shows the example of the test results using the recorded wave during Hyogo-ken Nanbu earthquake occurred in 1995 by horizontal and vertical excitations. During seismic response of the scale model, three-dimensional behavior like top-spinning was observed. However, the residual sliding displacements were very small (about 5mm). Maximum rotational response angle for original wave was about 0.417 rad., and the maximum uplifting displacement at the gravity center of the scale model cask was 26.5 mm.

Fig.13 shows the maximum rotational angle response of a scale model cask for four input waves. The increase of maximum response angle by the effect of the vertical motion was up to 20%. Moreover, as the power of the JMA Kobe wave was bigger than the other waves in low frequency region, the response for JMA Kobe wave excitation was much bigger than the one for the other wave excitations.

Fig.14 shows the influence of the gap between the canister model and the cask body on maximum rotational angle response of a scale model cask for the artificial wave type2. The existence of the gap between cask body and canister decreases the rotational angle response of the model cask.

In case of the artificial wave type 2, the rapid increase of the response angle beyond 1000gal was observed. Therefore, if the maximum input acceleration value and time duration of the wave is enough long, the tipping-over phenomena should be considered to investigate the integrity of the cask against overturning during strong earthquake motions.

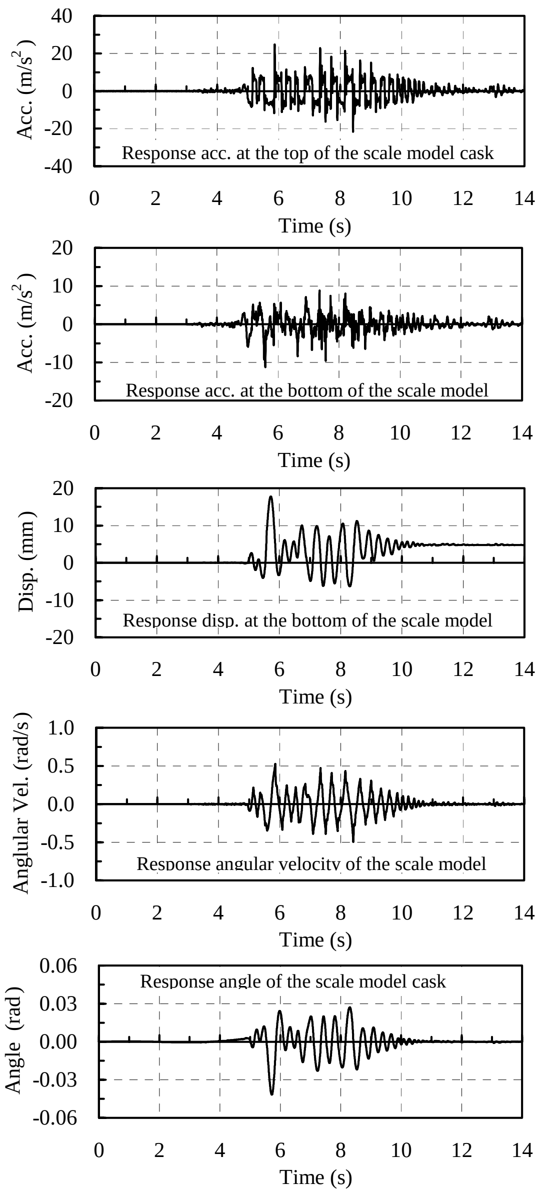

Fig.12 Example of time history for excitation test (JMA Kobe, horizontal and vertical excitation)

TIPPING-OVER CRITERIA BY ENERGY SPECTRUM

Energy Spectrum Approach

Akiyama et al. [4] proposed the estimation method for tipping-over of the two-dimensional rigid rectangular body as shown in Fig.14 based on the energy spectrum approach. The criteria for the tipping-over of this rigid body with energy spectrum are defined by equation (2).

$$_{ou}V_E(a) < V_{Ereq} \qquad (2)$$

V_{Ereq} is defined as the equivalent velocity calculated from the critical potential energy of the rigid body as defined by equation (3).

$$V_{Ereq} = \sqrt{2E_{req}/M} = \sqrt{2g\Delta H} = \sqrt{2ga(1-\sin\alpha)} = \sqrt{g(\sqrt{B^2+H^2}-H)} \qquad (3)$$

Akiyama et al. have also proposed the equivalent velocity calculated from input energy to rigid body as defined by equation (4). Notation in the equation (4) is designated in Fig.15. $V_{E0}(T)$ is the energy spectrum without damping. Fig.16. shows an example of the energy spectrum for JMA Kobe wave used in the excitation test.

$$_{ou}V_E(a) = \sqrt{\int_{T_0}^{T_1} f(T)(V_{E0}(T))^2\,dT} \qquad f(T) = -\frac{2(T-T_1)}{(T_1-T_0)^2} \qquad T_0 = 0.05\sqrt{a} \qquad T_1 = 0.5\sqrt{a} \qquad (4)$$

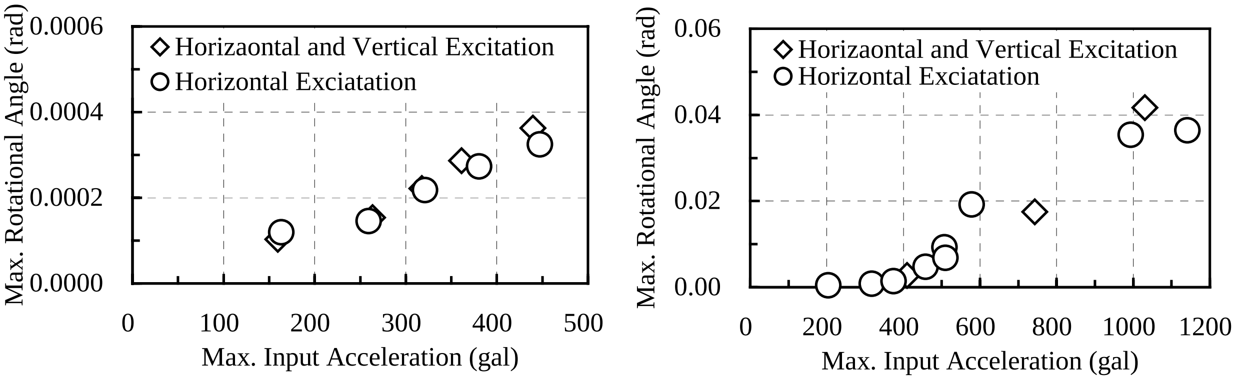

(El Centro) (JMA Kobe)

(Artificial Wave Type 1) (Artificial Wave Type 2)

Fig.13 Maximum rotational angle response of a scale model cask for excitation tests

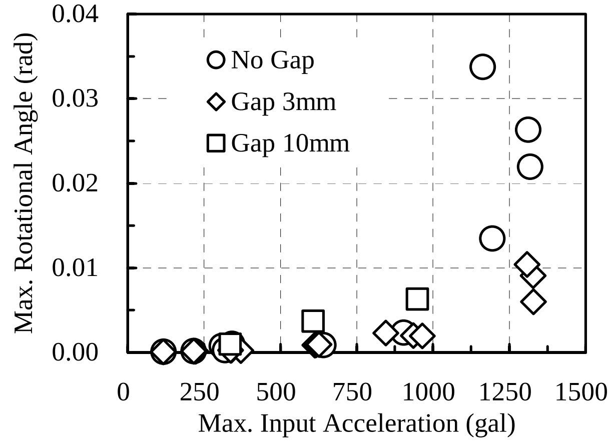

Fig.14 Influence of the gap between the canister model and the cask body (Artificial Wave Type 2)

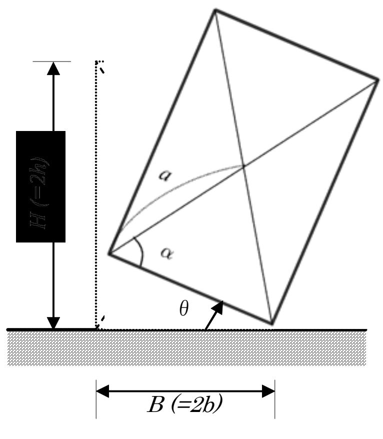

Fig.15 Two-dimensional rectangular rigid body

Fig.17 shows the relationship between the equivalent velocities for input energy and for potential energy necessary for uplifting the scale model cask during the excitation tests.

In case of JMA Kobe wave, as the input acceleration level increases, the experimental value is approaching to "${}_{ou}V_E=V_{Eresp}$-line", and all of the energy accumulated to the model cask by the earthquake wave is consumed for uplifting the model cask. On the other hand, as in case of the type2 wave, the experimental value is far from "${}_{ou}V_E=V_{Eresp}$-line", the energy approach may give too conservative estimation.

As a result, it is found that the energy spectrum criteria are very useful and practical to estimate conservatively the possibility of the tipping-over of the real cask during the storage subjected to the strong earthquake motions.

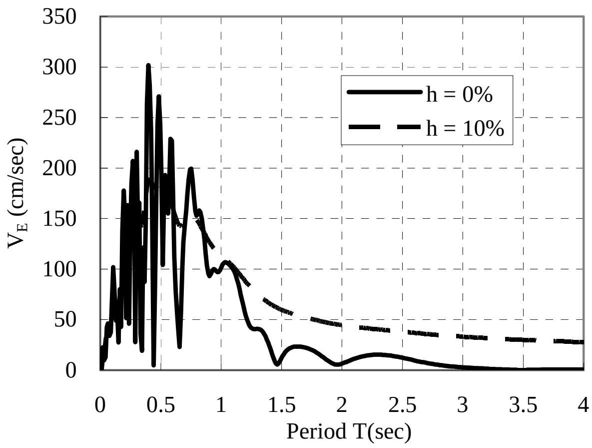

Fig.16 Energy spectrum for JMA Kobe wave

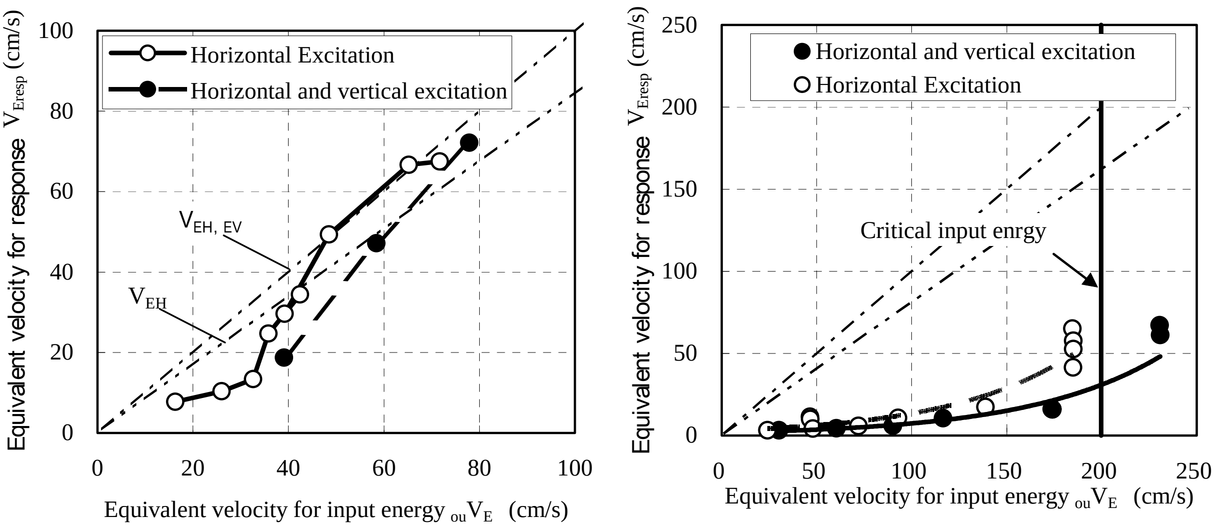

(JMA Kobe) (Artificial Wave Type 2)

Fig.17 Relationship between the equivalent velocities for input energy and for potential energy

CONCLUSION

Concrete cask spent fuel storage system is considered to essentially have an economical advantage and becoming widely used. For vertically free-standing concrete cask on the floor pad in the cask storage facility, its tipping-over and sliding behavior during earthquake is one of the technical key issues to guarantee its safe performance. To clarify the tipping-over characteristics of the cask, the experimental studies are performed by performing the excitation test with a scale model concrete cask using two dimensional shaking table. According to the test results, it is found that the tipping-over of the scale model cask was not observed even if the acceleration level which exceeds the ultimate input level as to the tipping-over derived by the energy approach or the tipping-over velocity criteria was loaded to the scale model cask. Moreover, to estimate the possibility of the tipping-over of the cask, the energy approach will be very useful and practical.

REFERENCES

1. Shirai K., Ito, C., Ozaki, S. and Ryu H., Development of Tip-over Analysis Code of Cask subjected to Strong Earthquakes, SMIRT12, Div. K., Stuttgart, Germany, Aug., 1993.
2. Ueno, M. and Shirai K., Demonstration program for qualification of concrete cask performance in CRIEPI, INMM Spent fuel Management Seminar XX, Washington, D.C., U.S.A., Jan., 2003.
3. Kaneko, M. and Hayashi Y., Proposal of a Curve to Describe Overturning Ratios of Rigid Bodies, J. Struct. Constr. Eng., AIJ, No.536, 55-62, Oct., 2000. (in Japanese)
4. Akiyama, H., Iyama, J. and Harada, Y., Estimate of Overturning of Rigid Bodies with Energy Spectrum, J. Struct. Constr. Eng., AIJ, No.488, 49-55, Oct., 1996. (in Japanese)